Development of Nanobiocomposite Fibers by Controlled Assembly of Rod-like Tobacco Mosaic Virus

Michael A. Bruckman · Zhongwei Niu · Siqi Li ·
L. Andrew Lee · Kris Varazo · Toby L. Nelson ·
John J. Lavigne · Qian Wang

Abstract One-dimensional composite nanofibers were generated via *in-situ* polymerization of polyaniline on the surface of tobacco mosaic virus (TMV) and the head-to-tail assembly of TMV. These composite nanofibers have very high aspect ratio and good processability. Two factors contribute to the formation of such TMV-composite fibers: (1) the accumulation and polymerization of monomers on the surface of TMV; and (2) the possibility of prolongation and stabilization of TMV helices. This strategy has been used in the synthesis of other polymeric bionanofibers with a variety of starting materials. In addition, the morphology of the final composite materials can be modulated by the covalent modification of TMV. When sulfonic acid groups are tailored to the exterior surface of TMV, polymerization of aniline can induce TMV to form branched structures with knot-like connections. On the other hand, modification of TMV with noncharged groups like acetylenes can block the assembly process completely. TEM and AFM are used to analyze the morphology and structure of composite fibers. This novel strategy to assemble TMV into 1D supramolecular assembly could be utilized in the fabrication of advanced materials for potential applications including electronics, optics, sensing, and biomedical engineering.

Introduction

Developing one-dimensional (1D) functional structures on nanometer scales defines a new paradigm in the fabrication of novel biomedical, optical, acoustic, electronic, and magnetic materials and devices [1–6]. In particular, the use of biological building blocks as templates in 1D material synthesis is an exciting and emerging area of research at the interface of biology, chemistry, and nanoscience [7–12]. Among many biological scaffolds, viruses and viral-like particles have recently attracted much attention as starting materials for the development of novel materials [8, 13–16]. Tobacco mosaic virus (TMV) is a classic example of a rod-like plant virus consisting of 2,130 identical protein subunits arranged helically around genomic single-RNA strand [17]. Native TMV particle is 300 nm long and 18 nm in diameter, with a 4-nm cylindrical cavity along the central core [18–20]. It has been shown that the surface properties of TMV can be manipulated chemically or genetically without disrupting the integrity and morphology of TMV capsids [21, 22]. The polar outer and inner surfaces of TMV have been exploited as templates to grow metal or metal oxide nanoparticles such as iron oxyhydroxides, CdS, PbS, gold, nickel, cobalt, silver, copper and iron oxides, and silica in many studies [13, 23–29]. For example, by varying the conditions of the deposition, it has been shown that one can either specifically decorate the external surface with metallic nanoparticles via the chemical reduction of $[PtCl_6]^{2-}$ or $[AuCl_4]^-$, or get constrained growth of Ag nanoparticles within the 4-nm internal channel present in the virus via the photochemical reduction of Ag salts [30,

M.A. Bruckman and Z. Niu contributed equally to this work.

M. A. Bruckman · Z. Niu · S. Li · L. A. Lee · T. L. Nelson ·
J. J. Lavigne · Q. Wang (✉)
Department of Chemistry and Biochemistry and Nanocenter,
University of South Carolina, 631 Sumter Street,
Columbia, SC 29208, USA
e-mail: wang@mail.chem.sc.edu

K. Varazo
Department of Chemistry, Francis Marion University, Florence,
SC 29501, USA

31]. Such 1D structures have already shown great potential with applications in nanoelectronics [32, 33].

In this paper, we present additional assembly pathways that can be achieved with TMV as the principle building block. Recently, we have reported that 1D polyaniline (Pani) fibers can be formed via *in situ* polymerization of aniline on TMV surface at neutral pH [34]. We have also adapted this strategy of long fiber formation towards the synthesis of other polymeric biocomposite nanofibers. In addition to the long fiber formations, extended incubation at low pH conditions can further induce these fibrous structures to assemble in a side-by-side manner to generate long bundled structures (Scheme 1, Path A). Furthermore, when sulfonic acids or other acidic groups are covalently attached to the exterior surface of TMV, polymerization of aniline induces TMV to form branched structures with knot-like connections (Scheme 1, Path B). Lastly, the modification of TMV with uncharged groups can block the 1D assembly completely, forming no observable long fibers (> 300 nm).

Experimental

General Reagents were used as received without further purification. Ultracentrifugation was performed at the indicated rpm values using a Beckman Optima™ L-90 K Ultracentrifuge equipped with either SW41 or 50.2 Ti rotors. All transmission electron microscopy (TEM) images were generated from a JEOL 100 CX II transmission electron microscope. Tapping-mode atomic force microscopy (AFM) images were obtained under ambient conditions using a NanoScope IIIA MultiMode AFM (Veeco). Silicon tips with a resonance frequency of approximately 300 kHz, a spring constant of about 40 N m^{-1} and a scan rate of 0.5 Hz were used.
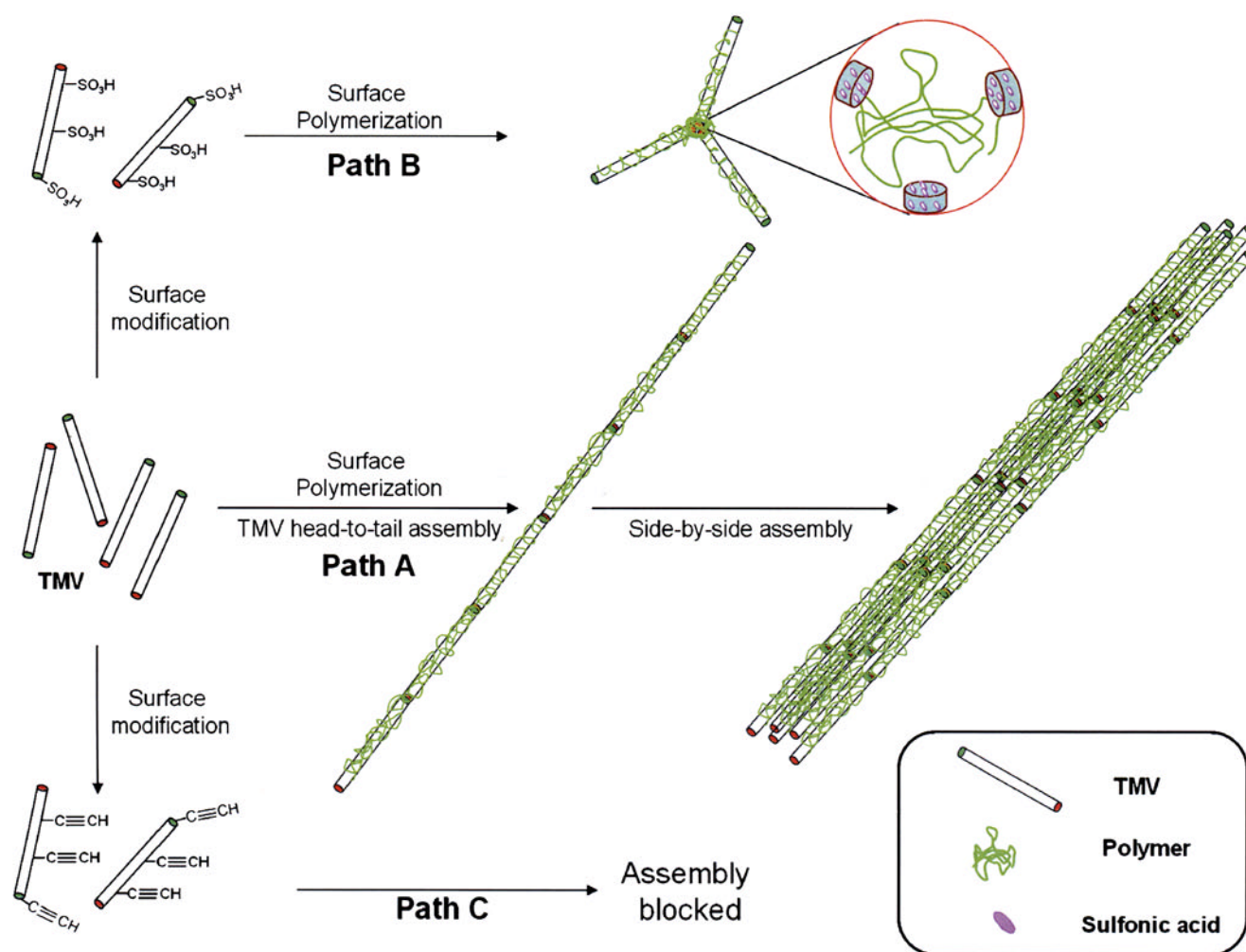
Scheme 1 Schematic illustration of the formation of TMV-templated nanoassemblies modulated by TMV surface modification and *in situ* surface polymerization.

Purification of TMV Tobacco plants approximately 1 month old were inoculated with TMV solution (0.025 mg/mL). The infected leaves were then harvested and stored frozen. For virus purification, the leaves were crushed and added to 10 mM potassium phosphate buffer at pH 7.8 with 0.2% β-mercaptoethanol. The mixture was centrifuged for 15 min before the supernatant was treated with a mixture of CHCl₃ and 1-butanol (v/v=1:1). The aqueous portion was separated and TMV was precipitated upon the addition of polyethylene glycol 8 K and NaCl. The resultant pellets were resuspended in 10 mM potassium phosphate buffer at pH 7.8. After a final round of ultracentrifugation at 42,000 rpm for 2.5 h with a Beckman 50.2 Ti rotor, pure TMV obtained as a clear pellet was resuspended overnight in 10 mM potassium-phosphate buffer at pH 7.8 or in pure water.

Surface Modification of TMV In a typical synthesis, diazonium salts were synthesized by mixing aqueous o-toluenesulfonic acid monohydrate (160 mg/mL, 200 μL), aqueous sodium nitrite (32 mg/mL, 200 μL) and 3-amino-benzosufonic acid (3) or 4-ethylnyl aniline (4) (10 mg/mL, 1.0 mL) at 0 °C for 1 h. A stock solution of TMV (15 mg/

mL, 2 mL) in 0.01 M phosphate buffer was diluted with aqueous borate buffer (150 mM, 5.2 mL, pH 8.8). To this solution, the diazonium salt solution prepared above was added. The reaction mixture was placed in an ice/water bath at around 4 °C for 3 h. Ultracentrifugation at 42,000 rpm for 2.5 h afforded a brown pellet, which was resuspended overnight in 10 mM phosphate buffers (pH 7.8) at 4 °C.

Synthesis of Methyl-Thiophen-3-yl-Ammonium Chloride (1) 3-Methylthiophene (10 g, 102 mmol) was dissolved in benzene (100 mL) then heated to reflux. The heating bath was removed and a mixture of N-bromosuccinimide (19 g, 107 mmol) and 2,2'-azobisisobutyronitrile (0.5 g) was added to reaction mixture. After the exothermic reaction subsided, the reaction mixture was refluxed for 3 h before it was cooled to room temperature. The solvent was removed and hexanes (1.7 L) added. The solution was filtered through a plug of silica gel to remove excess succinimide. The 3-bromomethylthiophene was purified by distillation (60 °C at ~1.0 torr) to yield a light yellow oil (14.9 g, 82% yield).

3-Bromomethylthiophene (7.8 g, 44.1 mmol) was dissolved in ethanol (50 mL) followed by 40% methylamine in
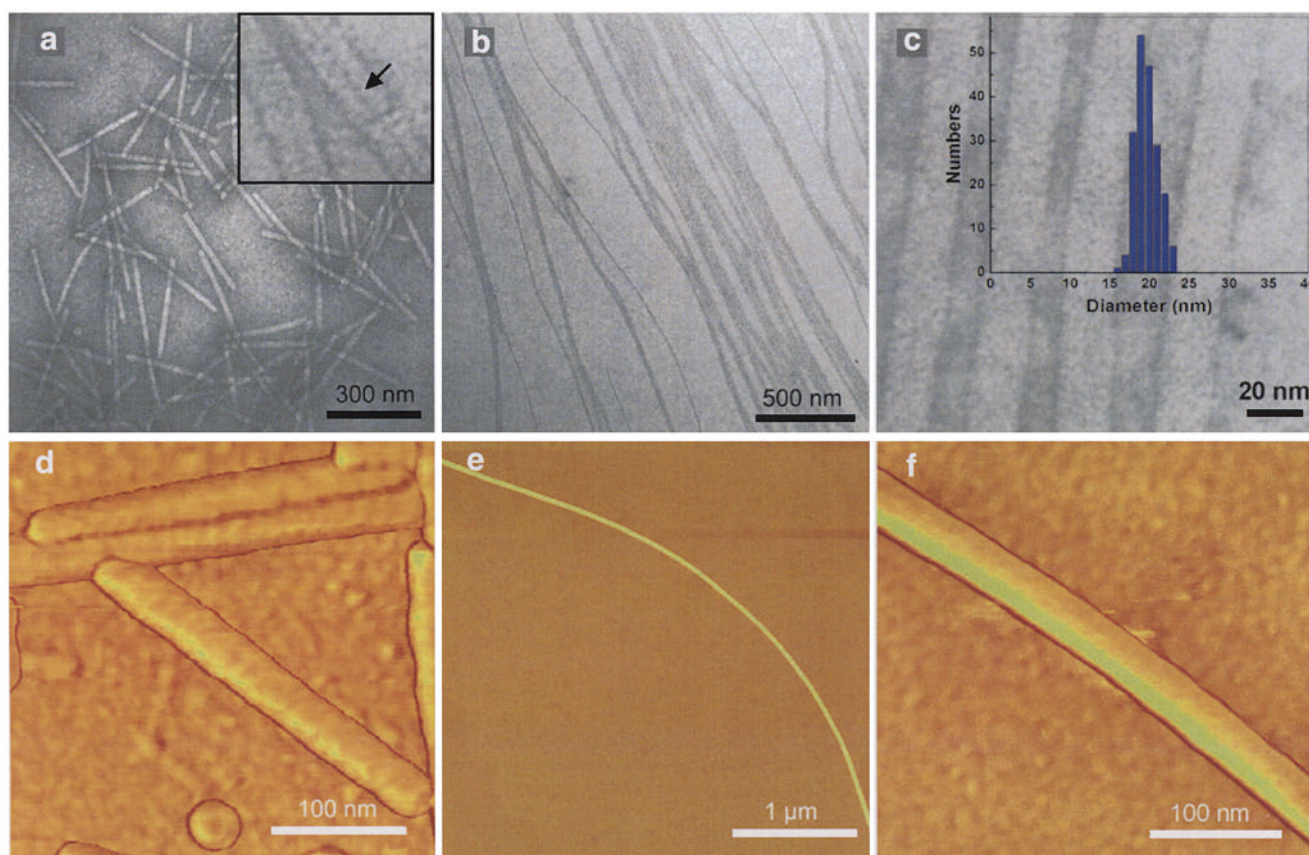
Fig. 1 (a) TEM image of wild-type TMV (inset: enlarged image of TMV. The internal channel is indicated by the arrow). (b) TEM image of PANI/TMV nanofibers. (c) An enlarged TEM image of PANI/TMV nanofibers (inset: size distribution of diameter of PANI/TMV nanofibers). (d) AFM phase image of wt-TMV. (e) AFM-phase image of PANI/TMV nanofibers. (f) An enlarged image of e.

water (30.3 mL, 352.5 mmol) was added. The reaction was stirred at room temperate for 3 h. After removal of solvents, ether (50 mL) and water (50 mL) were added. The aqueous layer was extracted twice with ether. The organic layers were combined, washed with brine, dried, filtered, and solvent removed. The resulting oil was dissolved in tetrahydrofuran (200 mL) and hydrochloric acid was added dropwise to give the final product as a pale white solid (7.0, 98% yield). ^{1}H NMR (300 MHz, D$_2$O): δ=2.57 (s, 3H), 4.12 (s, 2H), 7.06–7.08 (dd, 1H), 7.39-7.43 (m, 1H), 7.46 (m, 1H); ^{13}C NMR (75 MHz, D$_2$O): δ=131.15, 127.94, 127.89, 127.64, 46.77, 31.99; HR-MS: found m/z 128.0538; calculated for C$_6$H$_{10}$NS: m/z 128.0534 (M+H).

Synthesis of Polyaniline/TMV Composites In a typical synthesis, distilled aniline (10 μL) and ammonium

persulfate (APS, 10 mg/mL, 1 mL) were added to a solution of TMV (1 mg/mL, 4 mL). The pH of the solution was adjusted with HCl aq. (0.1 M) and NaOH aq. (0.1 M). The reaction mixture was incubated at room temperature for 24 h before it was centrifuged at 9,500 rpm for 15 min. The pellet was collected and immediately rinsed three times with pure water before resuspending in deionized water to give the pure polyaniline/TMV composite nanofibers. The synthesis of other polymer/TMV composite fibers followed the same protocol.

Preparation of Samples for TEM Analysis A solution of TMV or polyaniline/TMV composite nanofiber solution (20 μL) was deposited onto a 300-mesh carbon-coated copper grid for 2 min. The grid was then stained with 2% uranyl acetate before the TEM analysis.
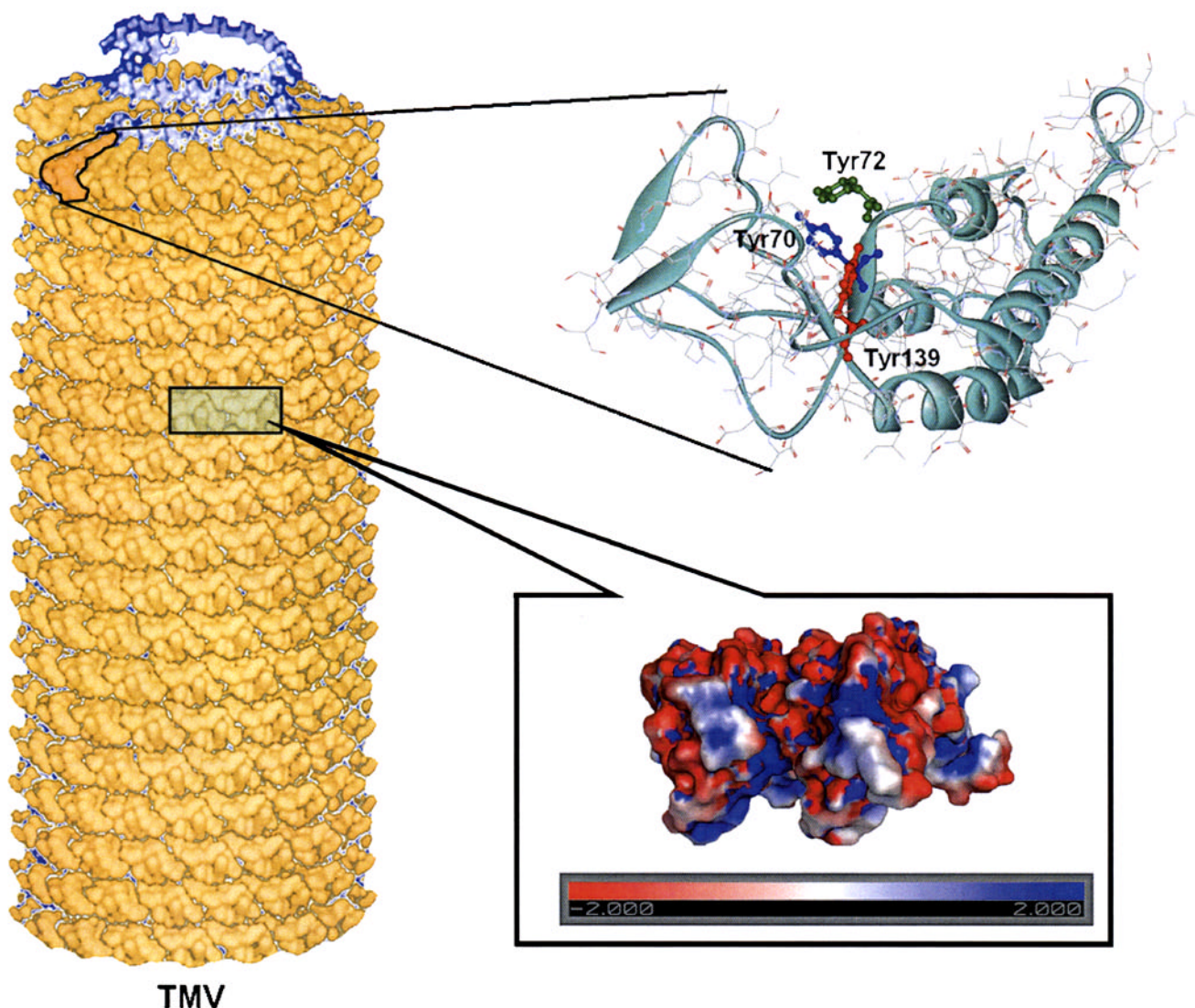
Fig. 2 (Left) Helical organization of TMV-coated proteins [18]. (Right-top) A single subunit structure of coat protein is presented as ribbon diagram with the reactive tyrosines being highlighted, among which Tyr-139 (in red) can be accessed from the side, but Tyr-70 (in blue) and Tyr-72 (in green) can only be accessed from the top face of the TMV particle. (Right-bottom) The surface charge distribution of the TMV-coated protein dimers is also shown (blue: positive; red: negative).

MALDI-TOF MS of TMV Subunit A solution of TMV (1 mg/mL, 26 μL) was treated with guanidinium-HCl (6.0 M, 4 μL) for 5 min at room temperature. The denatured protein was spotted onto a MALDI plate using Millipore ZipTip$_{\mu-C18}$® tips to remove the salts. The samples were analyzed using a Bruker Ultra-Flex I TOF/TOF mass spectrometer with MS grade sinapinic acid in 70% acetonitrile and 0.1% TFA as the matrix.

Results and Discussion

Synthesis of 1D Nanofibers (Scheme 1, Path A)

As shown in Fig. 1a, the diameter of native TMV is around 18 nm. After negative staining with 2% uranyl acetate, the 4-nm inner channel can be clearly visualized (Fig. 1a, inset). The length of native TMV, i.e., 300 nm, is defined by the encapsulated genomic RNA that stabilizes the coat protein assembly. A head-to-tail-ordered assembly of wild-type TMV has been observed, likely a product of complementary hydrophobic interactions between the dipolar ends of the helical structure [17]. A monomeric molecule with amino group(s) or positive-charged groups, such as aniline, can accumulate on the surface of TMV because of the electrostatic attraction or hydrogen bonding to the negatively charged surface residues. The local concentration of aniline on the TMV surface is much higher than that in solution; therefore, *in situ* polymerization should be able to produce a thin layer of polymer exclusively on the surface of TMV, and fix the head-to-tail-assembled tube-like structure. The intrinsic anisotropic morphology of PANI at diluted polymerization conditions further assisted the 1D nanofibers formation [35–39]. As shown by TEM and AFM, the length of the fiber can reach several micrometers (Fig. 1b and e).

After being coated with PANI on its surface, the diameter of TMV increased to 20 nm, which was measured with TEM (Fig. 1c). The inner channel could not be easily detected even after negative staining. Comparing to TEM images, AFM tapping mode phase images can give more detailed surface features. The surface of composite fiber becomes flatter and smoother compared with that of TMV particles (Fig. 1d and f). There is no visible gap that can be detected from a 4-μm composite fiber (Fig. 1e). This indicates that the head-to-tail protein–protein interactions lead to the formation of fiber-like structures. Such interaction, in principle, is identical to the subunit interactions at any cross-section of the native TMV [17, 40]. Therefore, there are two crucial factors that facilitate the formation of long 1D TMV-composite fibers: (1) accumulation and polymerization of monomers on the

surface of TMV; and (2) prolongation and stabilization of TMV helices.

As shown in Fig. 2, the exterior surface of TMV is highly charged and hydrophilic. In particular, the particles carry negative charges at neutral pH as the p*I* of TMV is around 3.5 [41]. The formation of TMV/PANI composite fibers is facilitated by the attraction of aniline (and also PANI) to the surface of TMV at neutral pH. Evidently, when thiophene was used as the monomer under a similar polymerization condition, no fiber-like structures were formed (Fig. 3a), likely because of the much weaker interaction between thiophene and the surface of TMV. An amino-functionalized thiophene salt, 1, was then synthesized as shown in Scheme 2. We hypothesized that the positively charged ammonium group will enhance the interaction of 1 with the negatively charged TMV surface. As shown in Fig. 3b, 1D long fibers were formed when a mixture of TMV and 1 was treated with APS. Similarly, no visible gap can be detected using TEM in such poly(3-aminothiophene)/TMV composite fibers (Fig. 3c). In addition to electrostatic interaction, hydrogen bonding can also increase the surface adsorption of monomers to TMV. For instance, when the polyethylene glycol methacrylate (PEG-MA, 2) was used as the monomer and ammonium persulfate was used as the initiator, the similar fiber-like structure could be readily obtained (Fig. 3d).

Surface Modification of TMV

Due to the helical organization of coat proteins, TMV can be assembled in a head-to-tail manner to form fiber-like structures [17, 40]. If the cross-section of TMV (the face normal to the helical axis) is modified, such kind of head-to-tail assembly should be twisted or blocked. To test this hypothesis, we further pursued the covalent surface modifications of TMV. It has been shown that phenol group of Tyr-139 can be readily accessed with an electrophilic substitution reactions at the ortho-position of the phenol ring in the presence of a diazonium salt [22]. This reaction can be efficiently used to insert desired functional groups using corresponding anilines to change viral properties such as solubility, surface charge, or surface functionality. In addition, modification of Tyr-139 does not influence TMV assembly [22]. On the other hand, although Tyr-70 and Tyr-72 cannot be accessed from the side surface of TMV, they are exposed on the top face (Fig. 2). Therefore, for any rod-like particle, there could be about 33–34 phenol groups belonging to Tyr-70, and Tyr-72, which can be modified on the top face. Still, such kind of top face modification could modulate the assembly pattern according to the properties of attached groups.

Using a modified protocol from literature [22], acidic or neutral groups were attached to the phenol groups of TMV

Fig. 3 TEM images of (a) TMV treated with thiophene and ammonium persulfate; no long fiber can be observed; (b) long fibers formed by mixing TMV with amino-functionalized thiophene 1 and ammonium persulfate; (c) an enlarged image of Fig. 2b; and (d) poly(PEGMA)/TMV composite fibers.
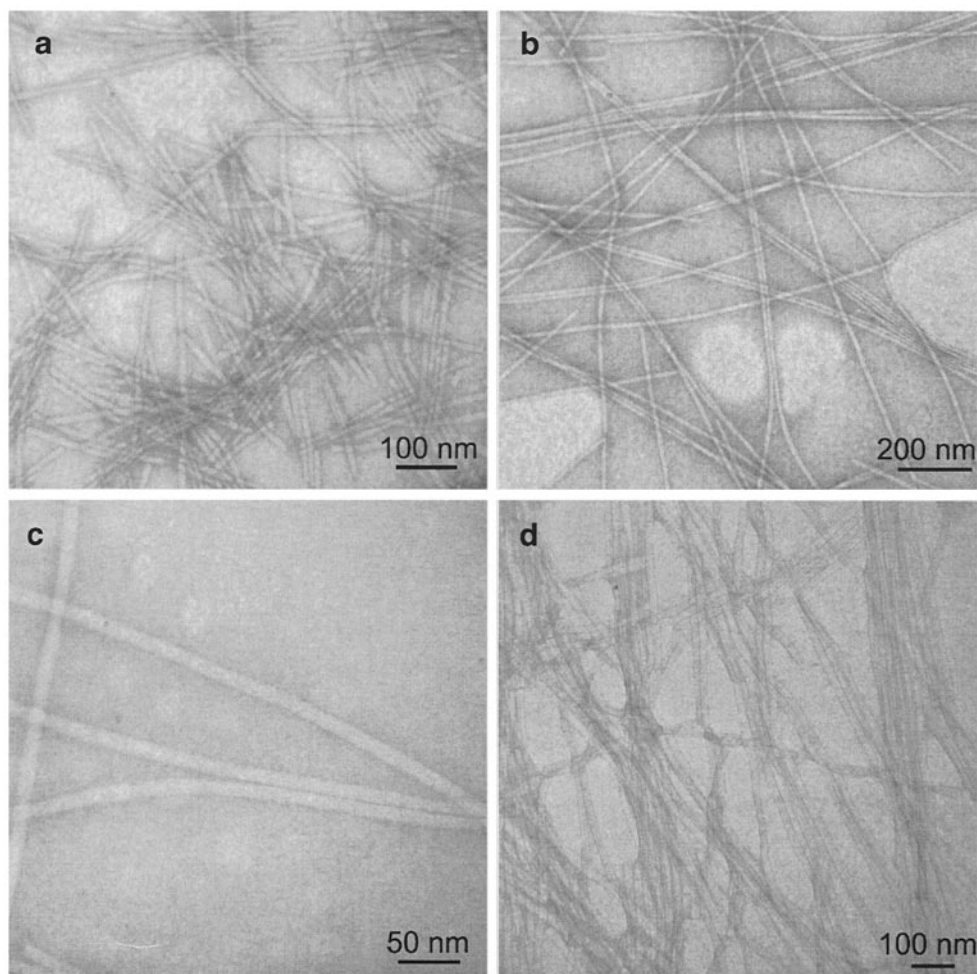
Scheme 2 Synthesis and structures of starting materials.
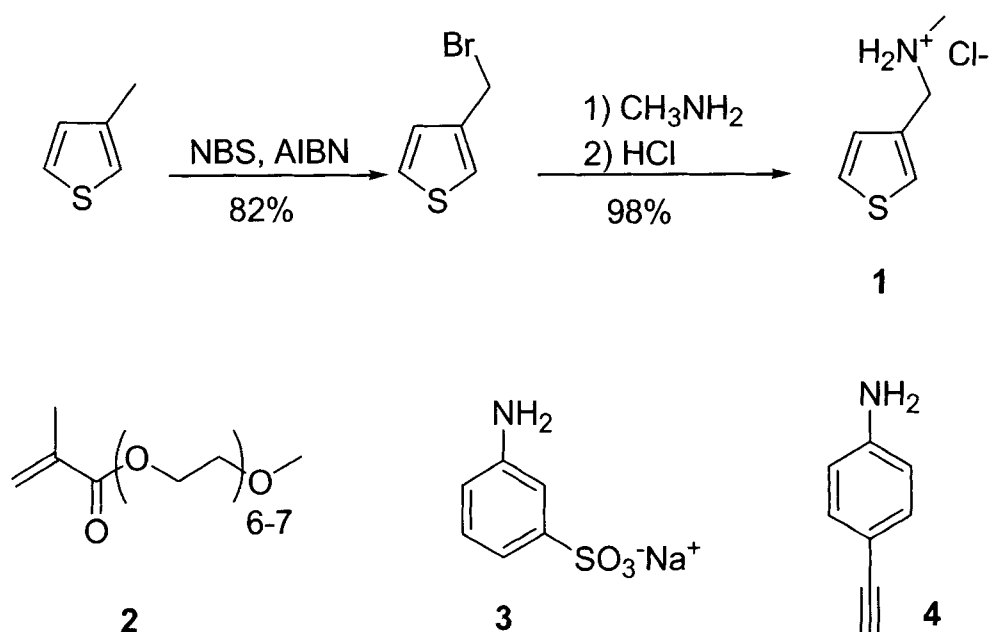
through a diazo linkage (Fig. 4a). The reactions were monitored using UV–Vis spectroscopy and MALDI-TOF MS. To force the modification of Tyr-70 and Tyr-72, large excess of diazonium reagents and extended reaction time were used. As shown in Fig. 4a, *meta*-aminobenzosulfonic acid (msa) **3** was converted into a diazonium salt using sodium nitrite in acidic solution, which reacted with TMV after incubation in a pH 9.0 buffer solution for 3 h. The formation of the diazo bond was monitored by the appearance of a broad absorption peak at about 324 nm in a UV–Vis spectrum (Fig. 4b). MALDI-MS analysis of the TMV-coated protein showed the molecular mass of the unmodified TMV subunit was 17,534 *m/z* (Fig. 4c). The mass of the product indicated that the majority of the protein subunits are modified with one msa group (17,711 *m/z*), along with small peaks at 17,534 *m/z* and 17,878 *m/z* that could be assigned to the unmodified and dual-modified protein subunits (or mono-modified protein subunits plus matrix peaks; Fig. 4c). Further tryptic digestion and MS analysis confirmed that the major

modification happened on Try-139. This result is consistent with the literature report [22]. Using para-ethynylaniline **4** as starting material to modify TMV, similar results were observed (data not shown).

Modulating the Assembly of PANI/TMV via Surface Modification

Introducing sulfonic acid groups to TMV should have two impacts on the final assembly process: (1) negative charges on the surface of TMV is increased that will lead to a stronger binding of aniline (as well as PANI) to TMV yielding nanofibers [42, 43]; and (2) the modification of the tyrosine residues will block the head-to-tail self-assembly of the TMV as the newly attached groups will hinder the subunits' interactions [44–46].

As shown by TEM, the surface modification does not affect the integrity of the TMV particles (Fig. 5a). However, after treating with aniline and ammonium persulfate, no
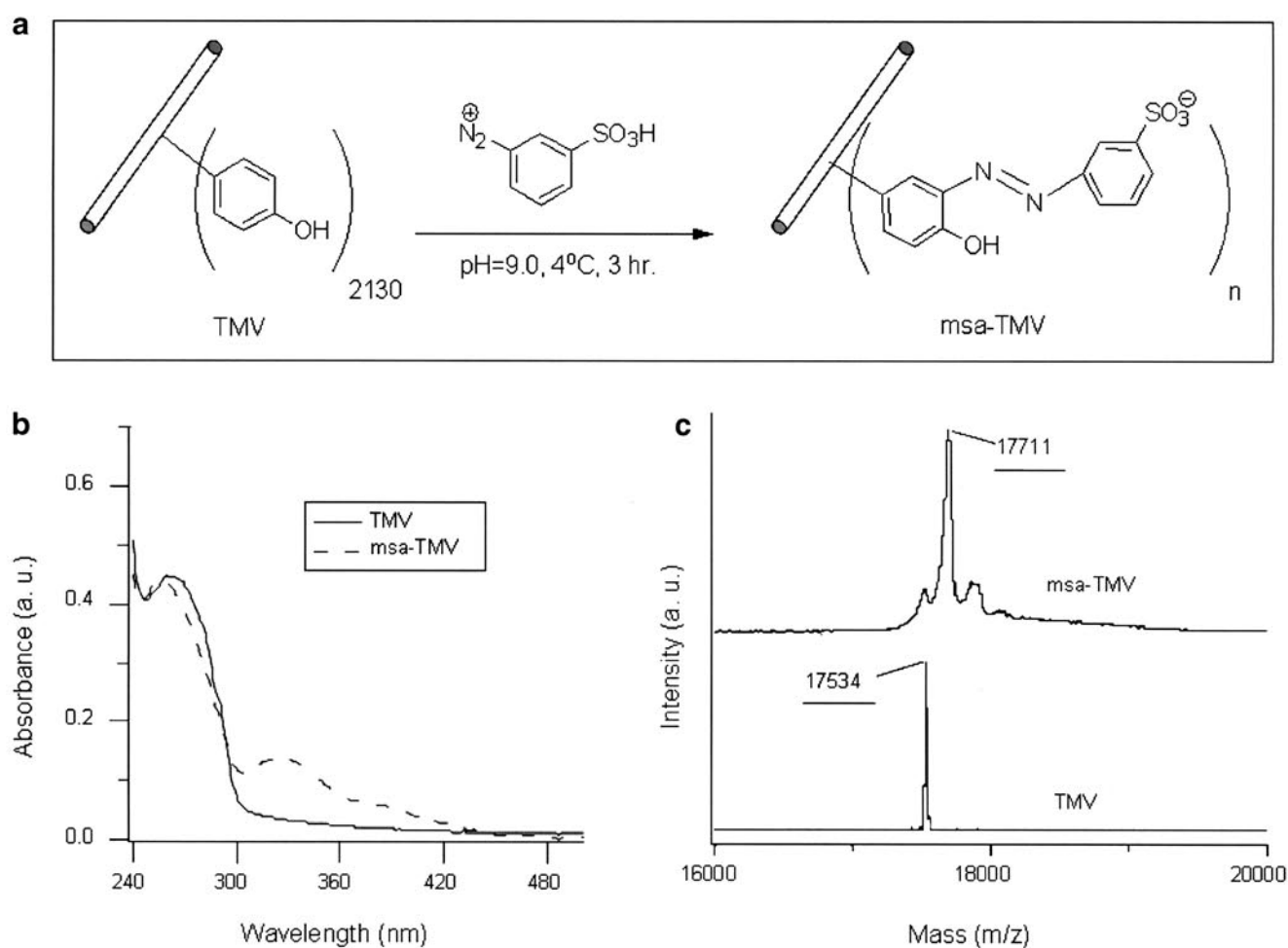
Fig. 4 (a) Reaction scheme leading to msa-modification of TMV (msa-TMV). (b) UV–Vis spectra of TMV and msa-TMV that shows characteristic absorbance peak at 324 nm. (c) MALDI-TOF MS of the coated protein of TMV and of the msa-TMV indicating single modification (17,693 *m/z*) of subunits.

Fig. 5 TEM images of (**a**) original msa-TMV, (**b** and **c**) TEM image of msa-TMV/PANI, and (**d**) alkyne-modified TMV treated with aniline and ammonium persulfate.
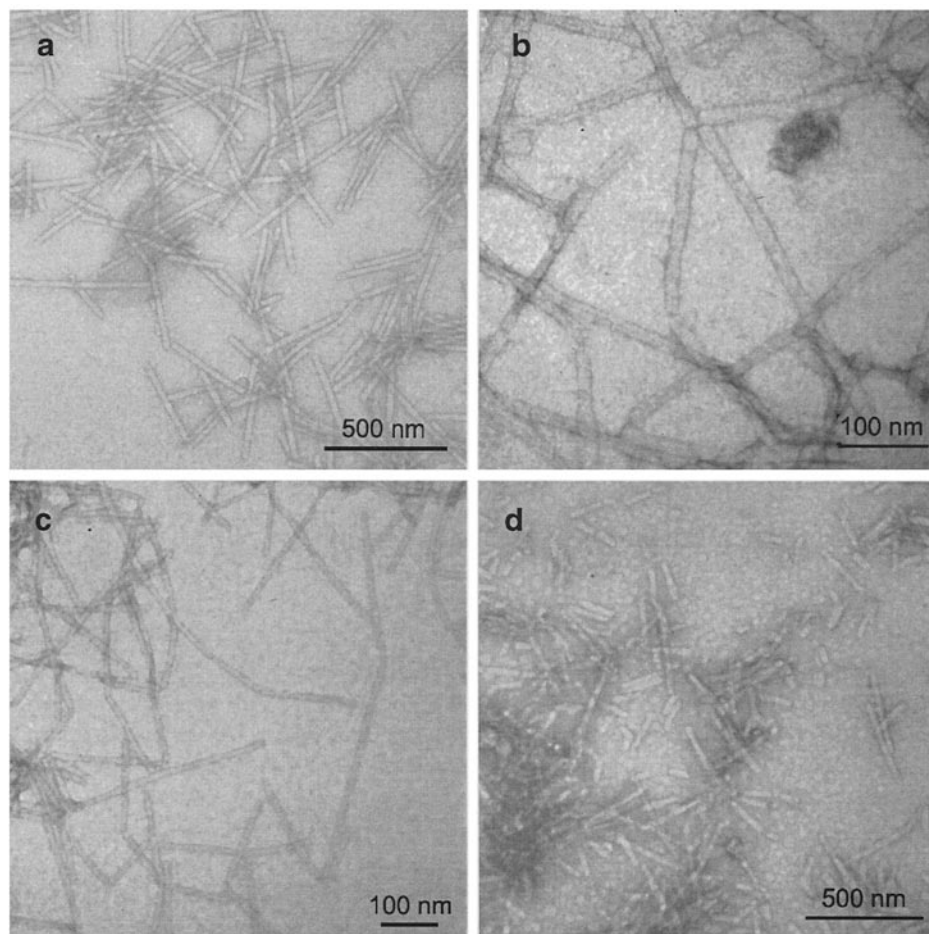
fiber-like structures were formed with sulfonic-acid-modified TMV (msa-TMV) as the starting material. The use of a negatively charged group did promote conglomeration at the ends of the particles. Branched structures with end-to-end knot-like connections were formed as the major morphology (Fig. 5b). Although long 1D fibers could also be observed occasionally, they always appeared as bended structures with gap between two TMV rods (Fig. 5c). Clearly, the end-face modification of TMV prohibited the perfect match of the helical prolongation as shown in Scheme 1 (Path A). Instead, the assembly of TMV/PANI adopted the Path B in Scheme 1. In addition, the additional acid groups on the end-face of TMV resulted in more PANI deposition, which served as the "glue" to connect TMV/ PANI rods together.

When alkyne-modified TMV particles were used as templates, the steric hindrance resulting from the compounds attached also blocked the assembly of TMV into long fibers. Furthermore, the noncharged alkyne groups could not attract the attachment of aniline or PANI as acidic groups did; therefore, it was difficult to have any PANI formed on the surface of alkyne tailored TMV particles. As

shown in Fig. 5d, the alkyne modified TMV, after being treated with aniline and ammonium persulfate, showed no difference from the started particles. Obviously, the assembly was completely blocked by the surface modification as illustrated as Path C in Scheme 1.

Conclusion

Well-understood structural information and availability of TMV, make this biological material an attractive starting scaffolding material for new materials development. We herein show that 1D polymeric composite fibers could be formed by the polymerization of a variety of monomers on the surface of TMV at neutral pH. The ability of TMV-coated proteins to form a regular helical array is the key that leads to an organized head-to-tail assembly as demonstrated by our results. Two factors particularly contribute to the formation of long 1D TMV-composite fibers: (1) the ability of accumulation and polymerization of monomers on the surface of TMV; and (2) the possibility of

prolongation and stabilization of TMV helices. Such composite nanofibers have very narrow dispersity in diameter, high aspect ratio, and excellent processibility. In addition, we demonstrate that the surface modification of TMV will modulate the assembly pattern and dictate the structures of the final composites. This strategy highlights the merit of developing novel nanomaterials using biological building blocks as templates and will promote many potential applications in optics, electronics, and biomedical engineering.

References

1. Cui Y, Lieber CM. Science 2001;291:851–53.
2. Huang Y, Duan X, Wei Q, Lieber CM. Science 2001;291:630–3.
3. Xia Y, Yang P, Sun Y, Wu Y, Mayers B, Gates B, et al. Adv Mater 2003;15:353–89.
4. Melosh NA, Boukai A, Diana F, Gerardot B, Badolato A, Petroff PM, et al. Science 2003;300:112–5.
5. Busbee BD, Obare SO, Murphy CJ. Adv Mater 2003;15:414–6.
6. Murphy CJ, Jana NR. Adv Mater 2002;14:80–2.
7. Niemeyer CM. Angew Chem Int Ed 2001;40:4128–58.
8. Flynn CE, Lee S-W, Peelle BR, Belcher AM. Acta Mater 2003;51:5867–80.
9. Seeman NC, Belcher AM. Proc Natl Acad Sci USA 2002;99:6451–5.
10. Seeman NC. Chem Biol 2003;10:1151–9.
11. Caswell KK, Wilson JN, Bunz UHF, Murphy CJ. J Am Chem Soc 2003;125:13914–5.
12. Dujardin E, Mann S. Adv Eng Mater 2002;4:461–74.
13. Shenton W, Douglas T, Young M, Stubbs G, Mann S. Adv Mater 1999;11:253–6.
14. Nam KT, Kim DW, Yoo PJ, Chiang CY, Meethong N, Hammond PT, et al. Science 2006;312:885–8.
15. Mao C, Solis DJ, Reiss BD, Kottmann ST, Sweeney RY, Hayhurst A, et al. Science 2004;303:213–7.
16. Lee LA, Wang Q. Nanomedicine 2006;2:137–49.
17. Klug A. Philos Trans R Soc Lond B Biol Sci 1999;354:531–5.
18. Stubbs G. Rep Prog Phys 2001;64:1389–425.
19. Jeng TW, Crowther RA, Stubbs G, Chiu W. J Mol Biol 1989;205:251–7.
20. Butler PJG, Lomonossoff GP. Biophys J 1980;32:295–312.
21. Yi H, Nisar S, Lee SY, Powers MA, Bentley WE, Payne GF, et al. Nano Lett 2005;5:1931–6.
22. Schlick TL, Ding Z, Kovacs EW, Francis MB. J Am Chem Soc 2005;127:3718–23.
23. Fowler CE, Shenton W, Stubbs G, Mann S. Adv Mater 2001;13:1266–9.
24. Fonoberov VA, Balandin AA. Nano Lett 2005;5:1920–3.
25. Royston E, Lee SY, Culver JN, Harris MT. J Colloid Interface Sci 2006;298:706–12.
26. Knez M, Bittner AM, Boes F, Wege C, Jeske H, Maiss E, et al. Nano Lett 2003;3:1079–82.
27. Knez M, Kadri A, Wege C, Gosele U, Jeske H, Nielsch K. Nano Lett 2006;6:1172–7.
28. Knez M, Sumser M, Bittner AM, Wege C, Jeske H, Martin TP, et al. Adv Funct Mater 2004;14:116–24.
29. Knez M, Sumser MP, Bittner AM, Wege C, Jeske H, Hoffmann DM, et al. Langmuir 2004;20:441–7.
30. Lee SY, Culver JN, Harris MT. J Colloid Interface Sci 2006;297:554–60.
31. Dujardin E, Peet C, Stubbs G, Culver JN, Mann S. Nano Lett 2003;3:413–7.
32. Tseng RJ, Tsai C, Ma L, Ouyang J, Ozkan CS, Yang Y. Nature Nanotechnology 2006;1:72–7.
33. Kalinin SV, Jesse S, Liu WL, Balandin AA. Appl Phys Lett 2006;88:153902.
34. Niu Z, Bruckman MA, Kotakadi VS, He J, Emrick T, Russell TP, et al. Chem Commun 2006; 3019–21.
35. Huang J, Virji S, Weiller BH, Kaner RB. J Am Chem Soc 2003;125:314–5.
36. Huang J, Kaner RB. J Am Chem Soc 2004;126:851–5.
37. Huang J, Kaner RB. Chem Commun 2006; 4:367–76.
38. Li D, Kaner RB. J Am Chem Soc 2006;128:968–75.
39. Chiou NR, Epstein AJ. Adv Mater 2005;17:1679–83.
40. Butler PJ. Philos Trans R Soc Lond B Biol Sci 1999;354:537–50.
41. Wadu-Mesthrige K, Pati B, McClain WM, Liu G-Y. Langmuir 1996;12:3511–5.
42. Wei Z, Wan M, Lin T, Dai L. Adv Mater 2003;15:136–9.
43. Liang L, Liu J, Windisch CF, Exarhos GJ, Lin Y. Angew Chem Int Ed 2002;41:3665–8.
44. Lu B, Taraporewala F, Stubbs G, Culver JN. Virology 1998;244:13–9.
45. Lu B, Stubbs G, Culver JN. Virology 1998;248:188–98.
46. Lu B, Stubbs G, Culver JN. Virology 1996;225:11–20.